Cell Reports, Volume *34*

Supplemental Information

Gain-of-function p53 protein transferred via small extracellular vesicles promotes conversion of fibroblasts to a cancer-associated phenotype

Shaolin Ma, Michael H. McGuire, Lingegowda S. Mangala, Sanghoon Lee, Elaine Stur, Wen Hu, Emine Bayraktar, Alejandro Villar-Prados, Cristina Ivan, Sherry Y. Wu, Akira Yokoi, Santosh K. Dasari, Nicholas B. Jennings, Jinsong Liu, Gabriel Lopez-Berestein, Prahlad Ram, and Anil K. Sood

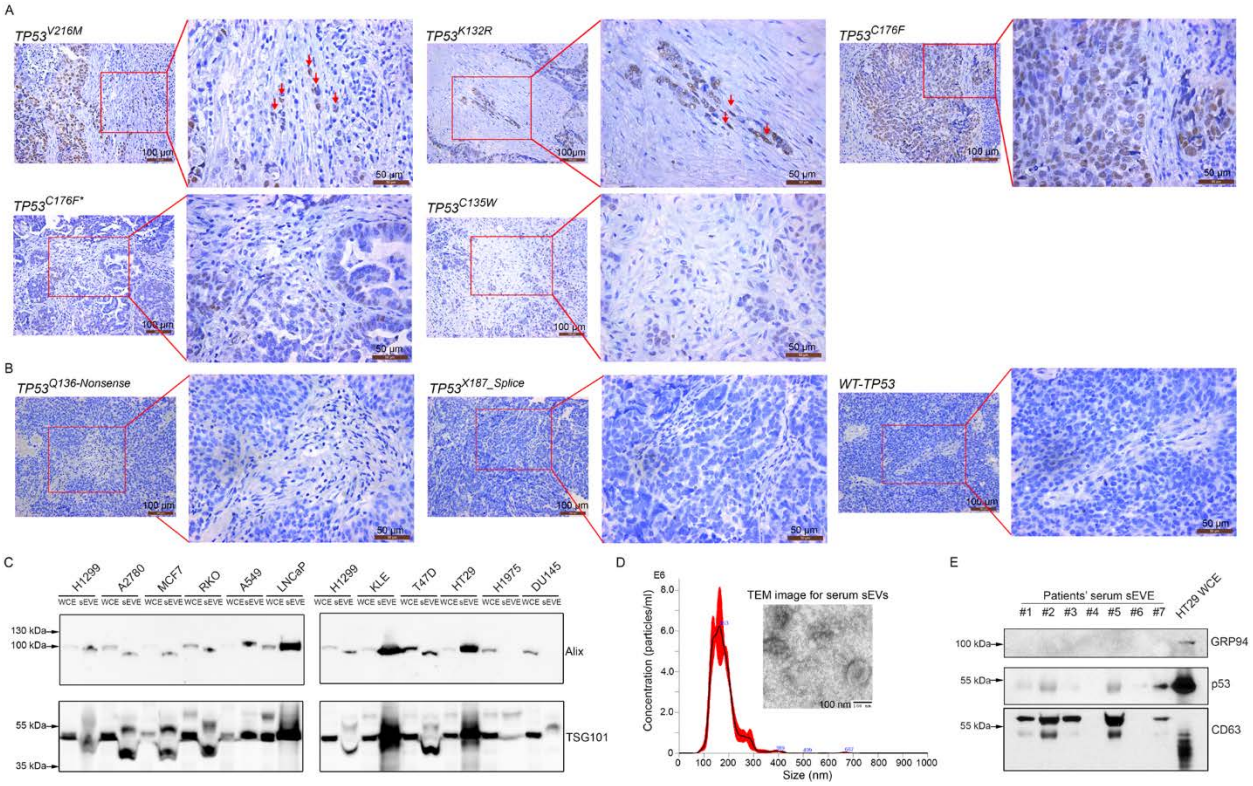

Figure S1. Presence of p53 protein in fibroblasts and small EVs of patient samples, Related to Figure 1

(A) Immunohistochemical staining for p53 in patient tumor with *TP53* mutations. Red arrows showing p53-positive fibroblasts. Scale bar, left, 100 μm; right, 50 μm. *, different patient.

(B) Immunohistochemical staining for p53 in patients with *TP53* nonsense mutation, a splice site mutation, or wt *TP53*. Scale bar, left, 100 μm; right, 50 μm.

(C) Expression of Alix and TSG101 of small EVs in a panel of 10 cell lines. H1299 is a p53-null cell line used as a negative control.

(D) Size of small EVs in serum as determined using Nano-tracking analysis (NTA). Transmission electron microscopy (TEM) image of small EVs isolated from serum samples. Scale bar, 100 nm.

(E) Presence of p53 protein in small EVs isolated from patient's serum. HT29 WCE was used as a positive control for GRP94.

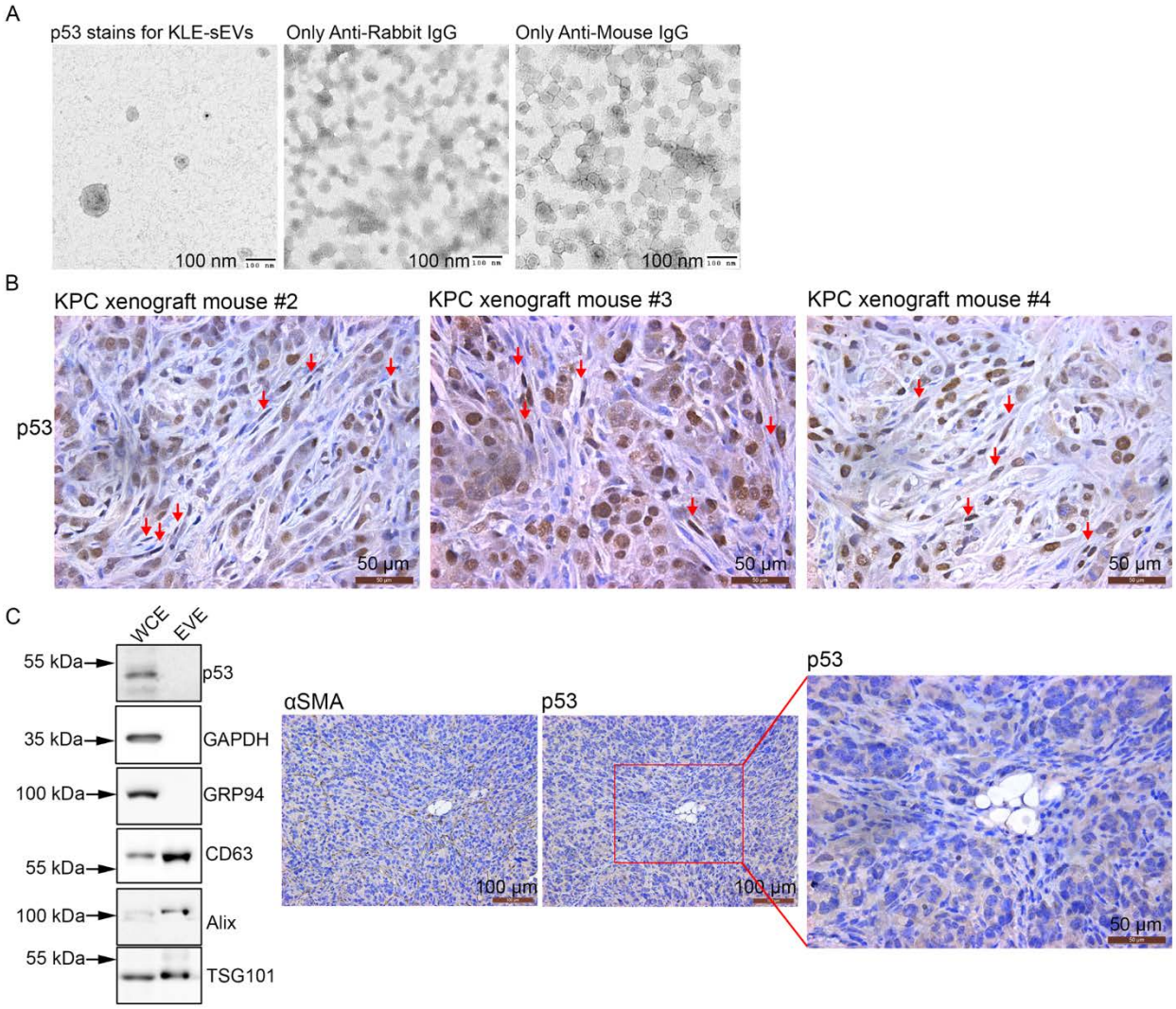

Figure S2. Negative controls for immune-gold assay and p53 expression in LSL *Trp53*$^{R172H/+}$ KPC and ID8 xenograft tumor tissues, Related to Figure 2

(A) Immuno-gold staining for p53 protein in KLE derives small EVs and negative controls. Scale bar, 100 nm.

(B) Immunohistochemical staining for p53 in other three *Trp53*$^{-/-}$ mice inoculated with LSL *Trp53*$^{R172H/+}$ KPC cells. Red arrows showing p53-positive fibroblasts. Scale bar, 50 μm.

(C) p53 expression in small EVs of ID8 cells and immunohistochemical staining for p53 in ID8 xenograft tumor tissue. Adjacent slides were used for staining p53 and αSMA. Scale bar, 100 μm and 50 μm.

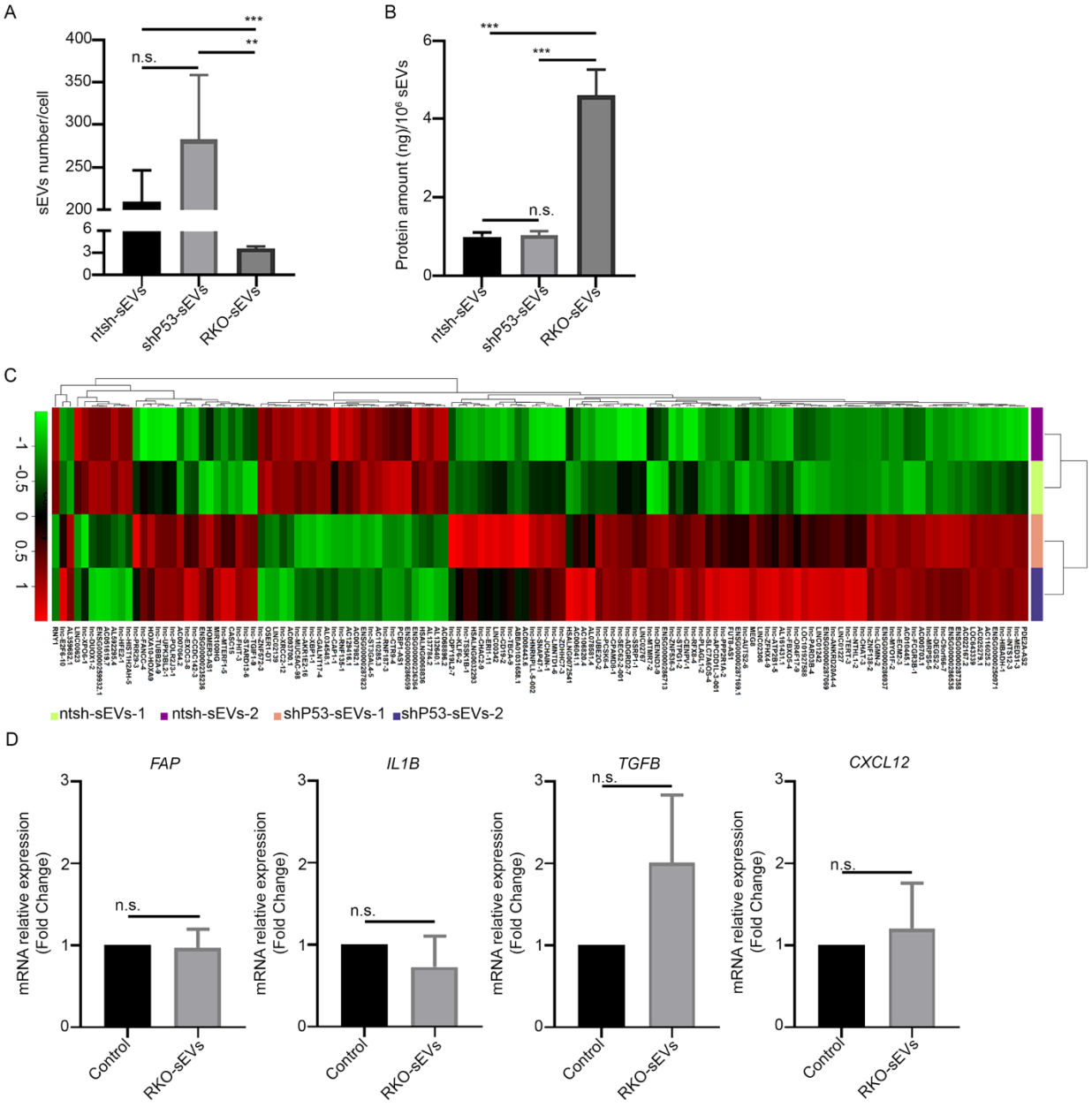

Figure S3. Comparison of small EVs in HT29-ntsh and -shP53 cells, Related to Figure 3

(A) Small EV secretion in HT29-ntsh, HT29-shP53, and RKO cells. Cells were cultured in Exo-depleted medium for 48 hr, and small EVs were harvested. Cells were counted after 48 hr of incubation. Data are represented as mean ± SD. **p < 0.01; ***p < 0.001; n.s., not significant.

(B) Amount of total protein carried in ntsh-sEVs, shP53-sEVs, and RKO-sEVs. Data are represented as mean ± SD. ***p < 0.001.

(C) A heatmap displaying the most differenced genes in ntsh-sEVs and shP53-sEVs.

(D) Expression of *FAP*, *IL1B*, *TGFB*, and *CXCL12* mRNA in NoF 151 fibroblasts after treatment with small EVs from RKO cells. Data are represented as mean ± SD. n.s., not significant.

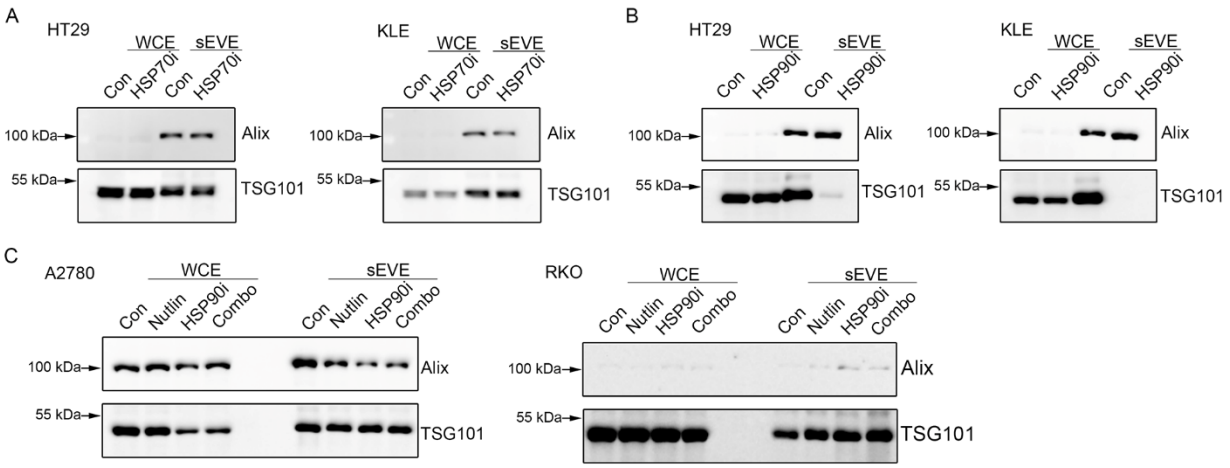

Figure S4. Expression of Alix and TSG101 in small EVs, Related to Figure 4

(A) Expression of markers for Alix and TSG101 in HT29- and KLE-derived small EVs after treatment with an HSP70 inhibitor (HSP70i). Con, control.

(B) Expression of markers for Alix and TSG101 in HT29- and KLE-derived small EVs after treatment with an HSP90 inhibitor (HSP90i).

(C) Expression of markers for Alix and TSG101 in A2780- and RKO-derived small EVs after treatment with nutlin-3A, HSP90i, or a combination of the two.

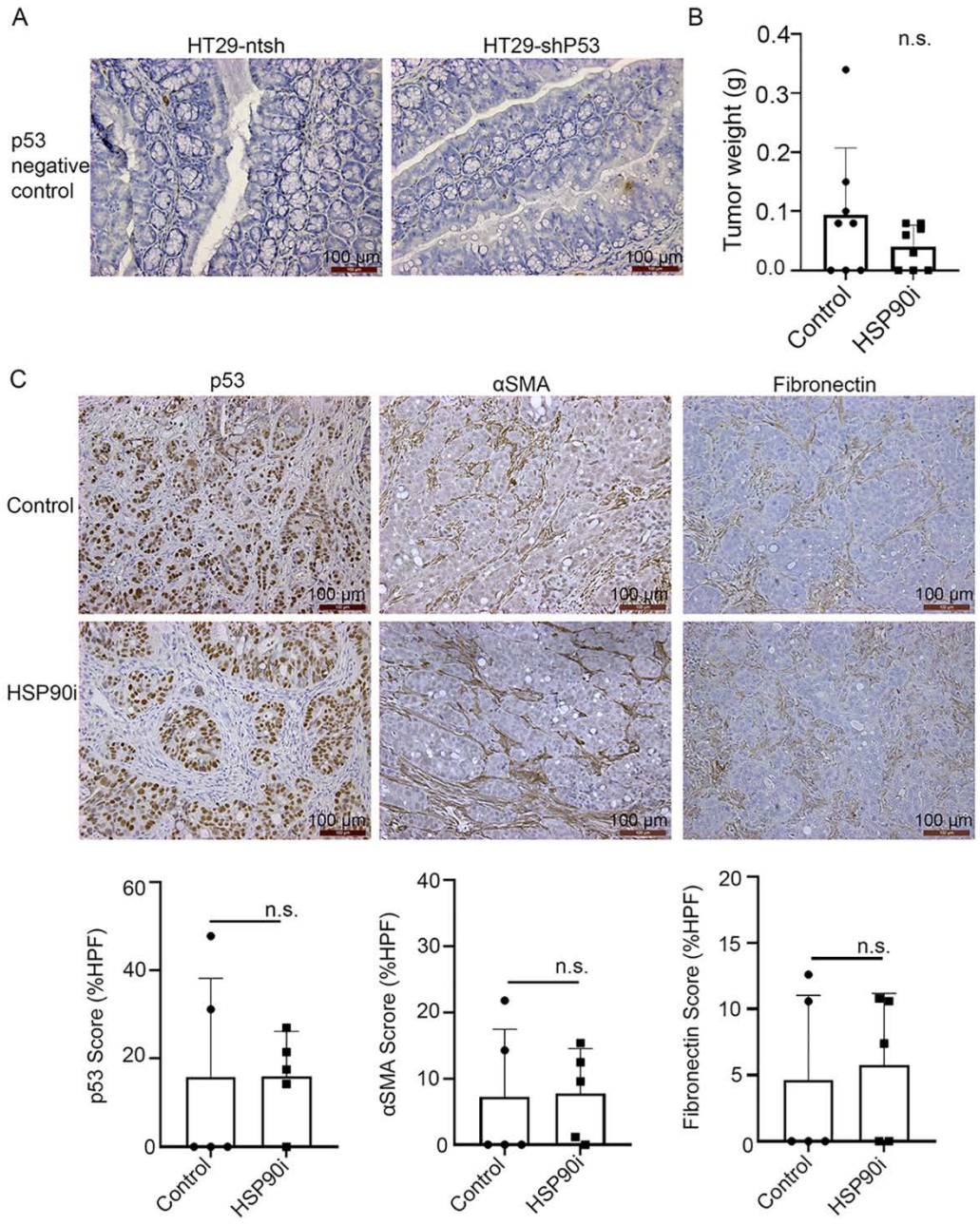

Figure S5. Effects of treatment with the HSP90 inhibitor 17-AAG on colorectal tumor growth and a CAF phenotype in an orthotopic mouse model, Related to Figure 5

(A) Immunohistochemical staining for cecum without tumor was provided as a negative control. Scale bar, 100 μm.

(B) Tumor weights and volumes in mice orthotopically inoculated with HT29 cells. Data are represented as mean ± SD. n.s., not significant.

(C) Comparison of p53, αSMA, and fibronectin expression based on IHC assay results in control and HSP90 inhibitor (HSP90i)-based treatment groups. The IHC score was determined based on the expression area and calculated using the IHC toolbox in the ImageJ software program. HPF, high-power field. Scale bar, 100 μm. Data are represented as mean ± SD. n.s., not significant.